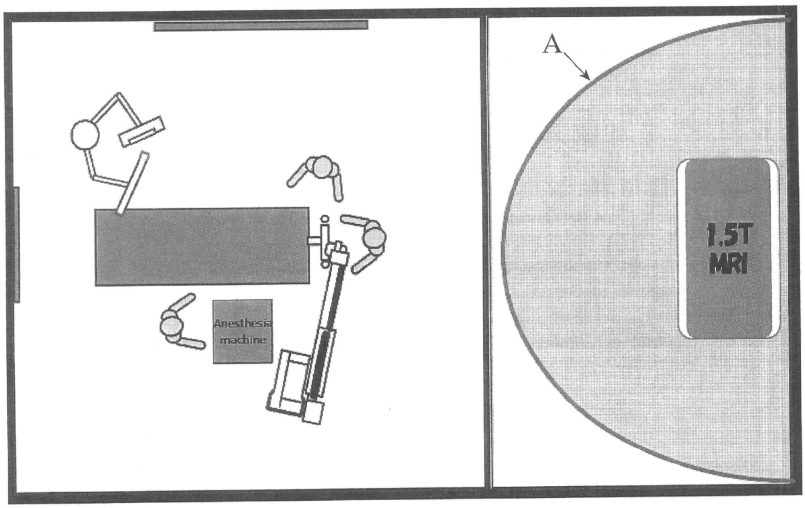

Fig. 1 Scheme of the new operation room. *line A* is 5-gauss line.

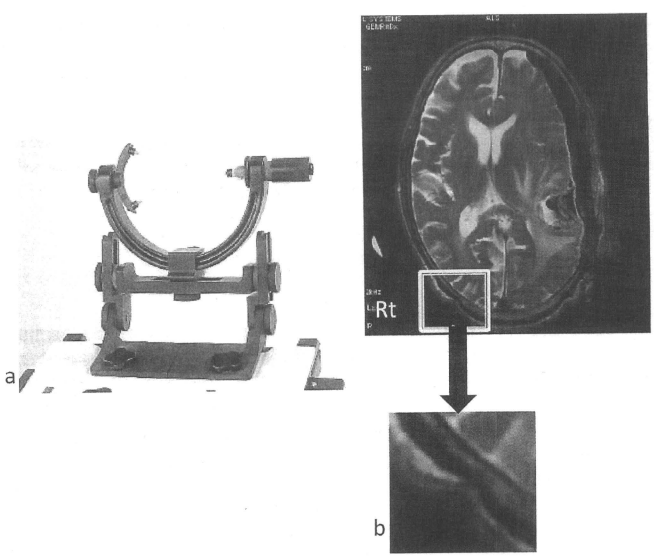

Fig. 2 **a**: Mayfield head clamp. **b**: MR image shows no artifact caused by head pin.

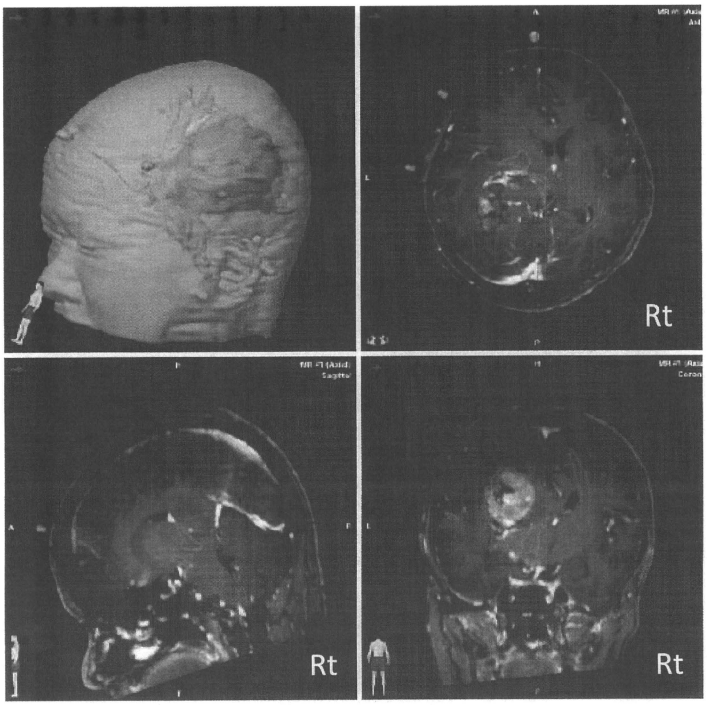

Fig. 3 T1-weighted images are displayed in axial, coronal and sagittal planes, as well as a 3-D rendering, depicting the three objects: tumor (*red*), fMRI (*yellow*), and pyramidal tract (*green*).

新手術室システム

当院に導入された術中MRIシステムは，いわゆるtwin-operating theaterといわれる形で，手術室とMRI検査室が2つの部屋に分かれている(**Fig. 1**)．このシステムの利点は，既存の手術器具をそのまま使用し従来とほぼ同じ環境で手術操作が可能，また手術患者の撮影を行っていないときには他の患者の検査が施行できるという経済的なメリットがある．しかしながら，MRIおよび手術室が一体となったシステムに比べ患者の移動距離が長くなるという不利な点もある．幸い当院では，麻酔科，その他co-medicalの理解と協力によりこれまで問題なく安全かつ迅速な患者移動および検査が行えている．MRIは1.5T(GE)の高磁場MRIが導入され，高磁場MRIによる精細な画像とMRA，MRS，tractographyなどの撮影が可能である．Neuronavigation (Brain Lab)は，院内の画像サーバーと術中MRIの両方から画像を取り込むことができ，術中画像は数分でナビゲーションシステムに転送され，再レジストレーションなく患者がMRI終了し手術再開までにup-dateが完了する．2009年4月より，術前に3.0T MRIで撮影したデータを用いて，術中fMRI，tractographyを合成する機能も追加となった．頭部固定は，カーボンファイバー製のメイフィールド3点固定装置でCT，angiography，MRIに対応している．ピンはサファイヤ製でMRIでもアーチファクトがほとんど生じない(**Fig. 2**)．術中蛍光診断システムとしては，KARL-STORZのFL400, FL800が，顕微鏡に搭載され，5-アミノレブリン酸による腫瘍蛍光診断と，ICGを用いた蛍光血管撮影が可能である．5-ALAの蛍光診断には，蛍光診断装置(M&M VLD-1)を用いてスペクトル解析も行い，肉眼では認識困難

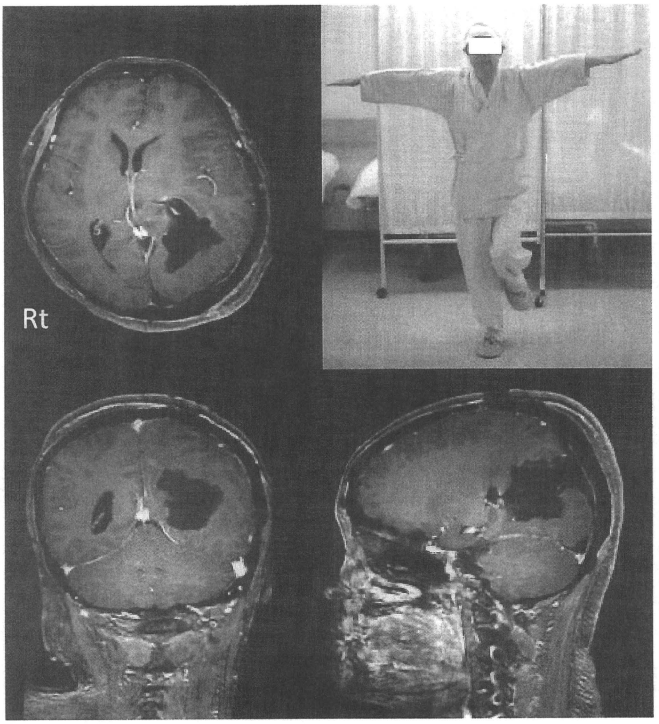

Fig. 4　Post-operative images show gross total removal of the tumor. Rt. motor weakness was improved after the operation.

な淡い蛍光を検出し腫瘍摘出度を向上させ局所再発率の低下を期待している.

対象と方法

2008年7月から2009年2月までに，32例の脳神経外科手術を施行した．内訳は，神経膠腫 14例，転移性脳腫瘍 3例，下垂体腺腫 7例，髄膜腫 3例，未破裂脳動脈瘤 3例，側頭葉てんかん（選択的海馬摘出術）2例，AVM 1例である．術中MRIシステムの最も良い適応は脳実質内腫瘍であるが，当科では腫瘍性病変以外の手術にも積極的に本システムを活用している．MRI検査は，DWI，T1, T2, FLAIR，造影3方向と脳動脈瘤・AVMではMRAも追加し，摘出率，虚血・出血病変などの有無の評価を行った．

症例呈示

症例1：54歳女性．Lt. parietal glioblastoma

右半身脱力と視野障害を主訴に来院した．MRIにてLt. parieto-occipitalに径5cmの腫瘍を認めた．Tractographyでは，錐体路は腫瘍により前方に圧排されていた．(**Fig. 3**) 開頭脳腫瘍摘出術を施行した．ナビゲーションにfMRIおよびtractographyデータを重ね，更にMEPによる運動モニタリングを併用し，腫瘍を全摘出した．術中MEPモニタリングで変化なく，MRIにて造影域の全摘出を確認して手術を終了した．術後，右片麻痺は消失した（**Fig. 4**）.

結　果

神経膠腫および転移性脳腫瘍17例の手術摘出率を示す.

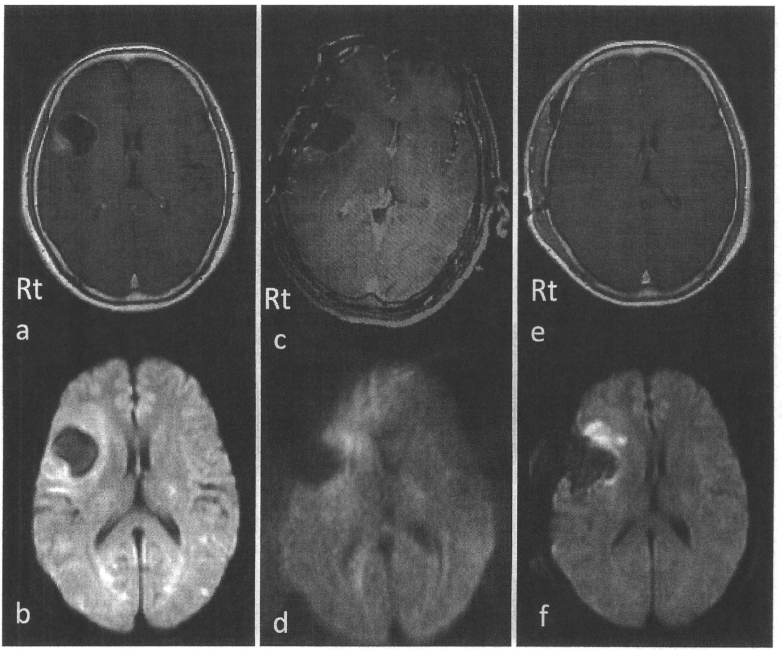

Fig. 5 Post-operative DW image revealed high signal area adjacent to the resection cavity (**e, f**). Intraoperative MR images do not show the abnormal intensity area (**c, d**). Preoperative MR images (**a, b**).

術中MRIにてGross total resection（GTR）は13例（76.5%）で得られた．術中MRI後に追加切除を加えた例は2例であった．脳梁を介して対側まで病変が及んでいた左前頭葉GBMと再発小脳GBMであり，摘出率の向上は得られたが，GTRまでは及ばなかった．術者がGTRと判断したにもかかわらず残存病変を認めた例はなかった．術中MRIの拡散強調画像にて，虚血病変を認めた症例はなかったが，術後MRIで腫瘍切断端にDWI高信号を認めた例が数例みられたことから，術中では手術操作から撮影までの時間が短く検出が困難であったと考えられた(**Fig. 5**)．出血に関しては，術翌日のCTにて摘出腔内に少量の出血を認めた鞍上部Glioma において，術中DWIにて同部位が高信号を呈していたことから，出血から撮像までの時間経過が影響するが，DWIにて術中の出血を検出できる可能性が示唆された(**Fig. 6**)．感染などの術中MRIに関連する合併症はこれまで認めていない．

考　察

術中MRIは，1993年ボストンのBrigham and Women's hospitalに世界に初めて導入され，その後世界各地で種々のシステムが開発され徐々に普及してきている[1)2)3)5)6)7)8)12)13)]．世界初のシステムは，0.3Tの低磁場MRIでコイルを縦に配置したDouble doughnut型といわれるもので，手術はコイルの間で行われ専用の手術器具を要するシステムである．日本でも同一システムが2000年に滋賀医科大学に日本初の術中MRIシステムとして導入された．同年，東京女子医科大学に導入されたシステムは，同じく低磁場MRIであるが，コイルを水平に配置し，手術を5ガウスラインより外側で行うことにより既存の手術機器がそのまま使用できるシステムである．また東京女子医科大学では，術中MRIだけではなく，ナビゲーションシステムおよび手術室情報管理システムを構築し，インテリジェント手術室という新たな概念を提唱した[15)16)]．2008年7月に稼働開始した当院

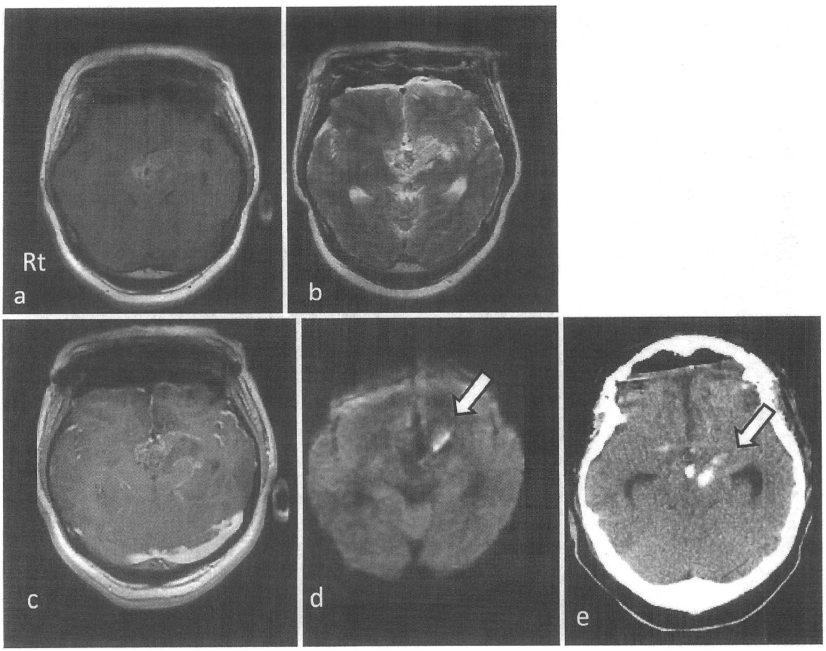

Fig. 6　Intraoperative MR images (**a**: T1-weighted, **b**: T2-weighted, **c**: T1 with Gadolinium, **d**: DWI). Intraoperative DW image shows intra-tumoral hemorrhage (**d**: *open arrow*). Post-operative CT shows the intra-tumoral hemorrhage (**e**: *open arrow*).

の新術中 MRI システムは国内 8 番目のものであり，高磁場 MRI システムとしては，2006 年の名古屋セントラル病院，東海大学についで日本で 3 番目となるものである[11][12]．

術中 MRI システムが脳神経外科手術にもたらす利点としては，brain shift を up-date し手術中の navigation の精度を上げ安全に腫瘍摘出率を向上させうるということ，また術野内・外の術中の予想外のイベントを察知できることがあげられる[4][17][18][20]．MRI による摘出率の判定を行うことにより，浸潤性に発育する glioma においても，手術摘出率が予後因子の 1 つであることが広く認められるようになり，術中 MRI システムを用いた摘出率向上は患者の予後向上に寄与するものと期待される[10][21]．実際に 2005 年 Claus らは，術中 MRI を用いて腫瘍摘出を行った場合に glioma 患者の予後改善がみられたことを報告している[4]．

術中 MRI は，すべての脳腫瘍手術に用いることが理想であるが，術中 MRI の必要度・貢献度は当然症例毎に異なる．また MRI のボアサイズ（患者撮影部位直径）による体位・頭位の制限もあり，現時点では全例に用いることは困難である．MRI のボアサイズ，コイル等の改良，頭部固定具，手術台の改良が必要である．

これまで悪性神経膠腫の摘出率の判定には，術後 48 時間以内の造影 T1 強調画像が用いられ，この判定に基づいた摘出率と予後との関係が検討されてきた．術中 MRI の自験例では，術中の trauma によっても造影剤漏出がみられることがあり，術中 MRI による残存腫瘍の判定に際して注意を要するものと考えている[9]．特に，腫瘍が正常脳に覆われて，正常脳が底になっている部位は顕微鏡の死角となりやすく腫瘍残存しやすい．また底となっている正常脳を脳ベラなどで移動することにより trauma が生じやすくこの部位から造影剤が漏出する可能性がある．腫瘍切除端の造影域が残存腫瘍であるのか，挫滅された脳なのか判断に注意を要する．術中画像のみにとらわれることなく，術前画像で in-

ternal controlとなる脳溝・動静脈などと腫瘍境界との関係をしっかり把握することが，術中MRI・ナビゲーションシステムを用いた手術でも重要である．

極めて浸潤能の高い悪性神経膠腫に対して，病理組織学的な全摘出を完遂することは難しい．しかし，治療後の再発のほとんどが局所再発であることから[9]，MRI造影病変の辺縁に存在する腫瘍細胞が高密度に浸潤していると考えられる部位をより多く摘出することが重要であると考えられる．MRI造影病変は色調や硬さなどによりある程度鑑別できるが，造影域辺縁の浸潤部位の最大限の摘出を目指す場合，術中MRIおよび術中蛍光診断の貢献度は大きいと考える．術中MRIシステムによる摘出率，治療成績の変化について検討するとともに，放射線・化学療法をはじめとする後療法の改良・開拓も今後の重要な課題である．

結　語

2008年7月，当科で1.5テスラ術中MRIシステム（1.5T MRI（GE），neuronavigation（Brain LAB），術中蛍光診断・術中血管撮影機能FL400, FL800（KARL-STORZ）搭載手術顕微鏡（Leica），MRI・CT対応operation table（MAQUET））を導入した．本新システムを使用して安全に脳神経外科手術を施行し，悪性脳腫瘍の70%以上でGross total removalがなされた．今後，他の脳神経外科手術への応用と悪性脳腫瘍の予後改善に対する本システムの有用性を検討したいと考えている．

文　献

1) Albayrak B, Samdani AF, and Black P: Intra-operative magnetic resonance imaging in neurosurgery. Acta Neurochir **146**: 543-557, 2004
2) Black PM, Alexander E 3rd, Martin C, et al: Craniotomy for tumor treatment in an intraoperative magnetic resonance imaging unit. Neurosurgery **45**: 423-430, 1999
3) Black PM, Moriarty T, Alexander E 3rd, et al: Development and implementation of intraoperative magnetic resonance imaging and its neurosurgical applications. Neurosurgery **41**: 831-845, 1997
4) Claus EB, Horlacher A, Hsu L, et al: Survival rates in patients with low-grade glioma after intraoperative magnetic resonance image guide. Cancer **103**: 1227-1233, 2005
5) Fahlbusch R, Ganslandt O, Buchfelder M, et al: Intraoperative magnetic resonance imaging during transsphenoidal surgery. J Neurosurg **95**: 381-390, 2001
6) Hall WA, Liu H, Maxwell RE, et al: Infuluence of 1.5-Tesla intraoperative MR imaging on surgical decision making. Acta Neurochir **85** (suppl): 29-37, 2002
7) Hall WA, and Truwit CL: Intraoperative MR-Guided Neurosurgery. J Magn Reson Imaging **27**: 368-375, 2008
8) Hushek SG, Martin AJ, Steckner M, et al: MR systems for MRI-Guided Interventions. J Magn Reson Imaging **27**: 253-266, 2008
9) Knauth M, Aras N, Rainer C, et al: Surgically induced intracranial contrast enhancement: potential source of diagnostic error in intraoperative MR imaging. AJNR **20**: 1547-1553, 1999
10) Lacroix M, Abi-Said D, Fourney DR, et al: A multivariate analysis of 416 patients with glioblastoma multiforme:prognosis, extent of resection, and survival. J Neurosurg **95**: 190-198, 2001
11) Maesawa S, Fujii M, Nakahara N, et al: Clinical indications for high-field 1.5T intraoperative magnetic resonance imaging and Neuro-navigation for neurosurgical procedures. Neurol Med Chir (Tokyo) **49**: 340-350, 2009
12) 松前光紀，厚見秀樹：画像誘導治療．脳神経外科 **35**: 329-342, 2007
13) Matsumae M, Koizumi J, Fukuyama H, et al: World's first magnetic resonance imaging/x-ray/operating room suite: a significant milestone in the improvement of neurosurgical diagnosis and treatment. J Neurosurg **107**: 266-273, 2007
14) McClain CD, Soriano SG, Goumnerova LC, et al: Detection of unanticipated intracranial hemorrhage during intraoperative magnetic resonance image-guided neurosurgery. J Neurosurg **106** (**5** Suppl Pediatrics): 398-400, 2007
15) 村垣善浩：術中MRI. NS Now **5**: 104-111, 2008
16) Muragaki Y, Iseki H, Maruyama T, et al: Usefulness of intraoperative magnetic resonance imaging for glioma surgery. Acta Neurochir Suppl **98**: 67-75, 2006
17) Nimsky C, Ganslandt O, Cerny S, et al: Quantification of, visualization of, and compensation for brain shift using intraoperative magnetic resonance imaging. Neurosurgery **47**: 1070-1080, 2000
18) Nimsky C, Ganslandt O, Hastreiter P, et al: Preoperative and intraoperative diffusion tensor imaging-based fiber tracking in glioma surgery. Nueurosurgery **56**: 130-138, 2005
19) Oppitz U, Maessen D, Zunterer H, et al: 3D-recurrence-pattern of glioblastomas after CT-planned postoperative irradiation. Radiotherapy and Oncology **53**: 53-57, 1999
20) Ozawa N, Muragaki Y, Nakamura R, et al: Shift of the Pyramidal tract during resection of the intraaxial brain tumors estimated by intraoperative diffusion-weighted imaging. Neurol Med Chir **49**: 51-56, 2009

21) The Comittee of the Brain Tumor Registry of Japan: Report of Brain Tumor Registry Japan (1984-2000), 12th ed. Neurol Med Chir (Tokyo) **49**: 1-101, 2009

Comments

著者らは，本論文にて高磁場 MRI 等を備えた統合型手術室を用いた脳腫瘍治療について，その有用性について記載した．手術手技，および手術支援装置の進歩にともなって，浸潤性の高い腫瘍である glioma においても，手術摘出の重要性の指摘がされてきている．より安全にかつ摘出度をあげるために，著者らは統合型手術室において，種々の工夫を行っている．本論文は将来の手術室の方向性を示し，またこのような手術室をあらたに設置しつつある者にとって，参考となる記載に富んだ論文である．

藤巻 高光（埼玉医科大学病院 脳神経外科）

術中 MRI 等を組み合わせたインテリジェント手術システムについての報告である．摘出度を上げると共に術後の神経症状の悪化を防ぎ，手術成績を向上するために様々な努力がなされて来たが，その最先端が結集されている．術中 MRI は腫瘍の摘出度を知る以外にも合併症の有無についての check もできる点で有用であるが，そのコストと移動や撮影に時間を要することが問題である．High-grade glioma の多くでは蛍光システムで代用出来るが，low-grade glioma などの造影を受けない病変での有用性は現在のところ他に変わるものはないだろう．多くの病院ではこのようにすべてをそろえることは不可能であり，どの機器がどのような手術の時に有用なのかを今後検証して行って欲しい．

中洲 敏（草津総合病院 脳腫瘍治療科）

Original Article

Benefits of Interferon-β and Temozolomide Combination Therapy for Newly Diagnosed Primary Glioblastoma With the Unmethylated MGMT Promoter

A Multicenter Study

Kazuya Motomura, MD[1]; Atsushi Natsume, MD[1,2]; Yugo Kishida, MD[1]; Hiroyuki Higashi[3]; Yutaka Kondo, MD[4]; Yoko Nakasu, MD[5]; Tatsuya Abe, MD[6]; Hiroki Namba, MD[7]; Kenji Wakai, MD[8]; and Toshihiko Wakabayashi, MD[1]

BACKGROUND: The aim of the current study was to catalog genomic and epigenomic abnormalities in newly diagnosed glioblastoma patients and determine the correlation among clinical, genetic, and epigenetic profiles and clinical outcome. **METHODS:** This study retrospectively included 68 consecutive patients who underwent surgical treatment and received standard radiotherapy with temozolomide (TMZ)-based chemotherapy. Of a total of 68 patients, 39 patients (57.4%) received interferon (IFN)-β in combination of TMZ. **RESULTS:** The genetic and epigenetic alterations frequently observed were *EGFR* amplification (51.5%), *TP53* mutation (33.8%), *CDKN2A* loss (32.4%), *TP53* loss (16.2%), methylation of the MGMT promoter (33.8%) and *IDH1* mutation (5.9%). Multivariate analysis revealed that methylated MGMT promoter and the combination of TMZ and IFN-β were independent prognostic factors associated with survival. The median survival time (MST) of the patients who received the combination of IFN-β and TMZ was significantly greater with 19.9 months as compared to the TMZ alone group (12.7 months). Notably, in even patients whose tumors had unmethylated MGMT promoter, the MST prolonged to 17.2 months when receiving TMZ with IFN-β, compared to 12.5 months in those receiving TMZ without IFN-β. **CONCLUSIONS:** Taken together, addition of IFN-β for newly diagnosed primary GBM achieved a favorable outcome, particularly in patients with unmethylated MGMT promoter. ***Cancer* 2010;000:000–000.** © *2010 American Cancer Society.*

KEYWORDS: IDH1, MGMT methylation, glioblastoma, interferon-β, temozolomide.

Glioblastoma multiforme (GBM) is one of the most frequent primary brain tumors in the central nervous system in adults and is highly malignant, with a median survival time of about one year from diagnosis. This is despite aggressive treatment, surgery, postoperative radiotherapy, and adjuvant chemotherapy. An international randomized trial by the European Organization for Research and Treatment of Cancer/National Cancer Institute of Canada (EORTC/NCIC) comparing radiotherapy alone and concomitant radiotherapy and temozolomide (TMZ) clearly attested the benefits of adjuvant TMZ chemotherapy for GBM patients.[1] Since then, TMZ has been the current first-line chemotherapeutic agent for GBM.

A subanalysis in this trial showed the effectiveness of epigenetic silencing of the MGMT gene by promoter methylation with longer survival in patients with primary GBM; it also suggested the benefits of combining chemotherapy using TMZ with radiotherapy.[2]

Corresponding author: Atsushi Natsume, MD, PhD, Department of Neurosurgery, Center for Genetic and Regenerative Medicine, Nagoya University School of Medicine, 65 Tsurumai-cho, Showa- ku, Nagoya 466-8550, Japan; Fax: (011) 81-52-744-2360; anatsume@med.nagoya-u.ac.jp

[1]Department of Neurosurgery, Nagoya University School of Medicine, Nagoya, Japan; [2]Center for Genetic and Regenerative Medicine, Nagoya University School of Medicine, Nagoya, Japan; [3]FALCO biosystems, Kyoto, Japan; [4]Division of Molecular Oncology, Aichi Cancer Center Research Institute, Nagoya, Japan; [5]Department of Neurosurgery, Shizuoka cancer center, Shizuoka, Japan; [6]Department of Neurosurgery, Oita University School of Medicine, Oita, Japan; [7]Department of Neurosurgery, Hamamatsu University School of medicine, Hamamatsu, Japan; [8]Department of Preventive Medicine/Biostatistics and Medical Decision Making, Nagoya University School of Medicine, Nagoya, Japan

We thank Mr. Akiyoshi Sakai (Clinical Laboratory, Kariya Toyota General Hospital, Kariya, Japan), Mr. Hideaki Maruse, Mr. Takafumi Fukui, and Mr. Yosuke Furui (FALCO biosystems, Kyoto, Japan) for wonderful technical assistance.

DOI: 10.1002/cncr.25637, **Received:** April 22, 2010; **Revised:** July 14, 2010; **Accepted:** August 2, 2010, **Published online** in Wiley Online Library (wileyonlinelibrary.com)

Furthermore, there have been recent attempts to comprehensively profile GBM genes by The Cancer Genome Atlas (TCGA) project and other groups.[3,4] Some genetic aberrations in GBM, such as *TP53* mutation or deletion, *NF1* deletion or mutation, and *ERBB2* mutation, have been found to be more common than previously reported. In addition, novel molecular markers, such as frequent mutations of the *IDH1* and *IDH2* genes in secondary GBM have been discovered.[5-7] These findings on mutations, genomic and epigenomic aberrations, and transcriptomal features in GBM might aid in understanding the classification of GBM and its further potential clinical implications.

However, the TCGA project included GBM patients who received surgical treatment, and detailed information on adjuvant chemoradiotherapy was not provided. Therefore, the close relationship between the gene profile provided by TCGA and chemotherapy regimens remains unknown.[3]

In this current study, we aimed to determine the correlation between clinical, genetic, and epigenetic profiles, and clinical outcome in newly diagnosed GBM patients who received TMZ-based chemotherapy. Interestingly, we found a significant beneficial outcome in patients receiving TMZ in addition to IFN-β. Moreover, our study discovered that GBM patients with the ummethylated O^6-methylguanine-DNA methyltransferase (MGMT) promoter, in particular, showed benefits from IFN-β.

MATERIALS AND METHODS

Patient population

We retrospectively reviewed 68 consecutive patients with newly diagnosed primary GBM who underwent surgical treatment at several academic tertiary-care neurosurgical institutions: Nagoya University Hospital, Hamamatsu University Hospital, Oita University Hospital, and Shizuoka Cancer Center from May 2006 through June 2010 after TMZ was approved as the treatment agent for malignant gliomas by the National Ministry of Health and Welfare of Japan. The diagnosis of GBM was established by histological confirmation according to the WHO guidelines[8,9] independently by at least two expert neuropathologists. The clinical, operative, and hospital course records were reviewed. Information collected from clinical notes included patient demographics, pre- and postoperative neuroimaging, and adjuvant therapy. Preoperative Eastern Cooperative Oncology Group performance status (ECOG PS) scores were assigned by the clinician at the time of evaluation and were available in the chart for review for all patients. The study was approved by the institutional review board at each participating hospital and complied with all provisions of the Declaration of Helsinki.

Treatment

Radiotherapy

After undergoing surgery, the patients received focal external-beam radiotherapy by conventional radiation planning to approximately 60 Gray (Gy) (±5% total dose), with daily concurrent TMZ at 75 mg/m^2 throughout the course of radiotherapy.

Chemotherapy

All patients received the standard Stupp regimen.[1] In the absence of grade 3 or 4 hematological excessive toxicity, TMZ administration was continued until clinical or radiological evidence of disease progression was observed. Of these 68 patients, 39 patients (57.4%) received adjuvant IFN-β treatment (Table 1). Patients in Nagoya University and Oita University received chemotherapy consisting of IFN-β. There were no significant differences in any of the clinical parameters and genetic, epigenetic parameters (i.e., age, sex, preoperative PS, tumor location, extent of resection, genetic and epigenetic alterations between the institutions using regimen with and without IFN-β. The IFN-β chemotherapy regimen comprised 3 million international units (MIU)/body administered intravenously on alternate days during radiotherapy and TMZ-induction chemotherapy.[10,11] At the end of the induction period, after a 4-week interval, the patients were administered 3 MIU/body of IFN-β on the first morning every 4 weeks during TMZ maintenance chemotherapy. In the case of tumor progression, salvage or second-line therapy was administered at the investigators' discretion; most patients received additional chemotherapy.

Response Evaluation During Treatment

Both radiological and clinical findings were used to evaluate the response. Follow-up magnetic resonance imaging (MRI) was performed for alternate cycles. If the MRI showed continued increase in enhancement, the case was considered as tumor progression. If re-resection was performed for a recurrent mass lesion, histological interpretation formed the basis for definitive diagnosis (treatment-related necrosis vs recurrent tumor).

Table 1. Clinical Characteristics[a]{TC}

Parameter	No. of Patients	%
	n=68	
Age(y)		
Median	55.0	
Range	12-84	
<40	12	17.6
≥40, <60	24	35.3
≥60	32	47.1
Sex		
Male	41	60.3
Female	27	39.7
Preoperative ECOG performance status		
Median	1	
Range	0-3	
Preoperative ECOG performance status		
≤1	45	66.2
>1	23	33.8
Tumor location		
Superficial	50	73.5
Deep	18	26.5
Surgery		
GTR	24	35.3
Non-GTR	44	64.7
Chemotherapy		
TMZ only	29	42.6
TMZ+ IFN-β	39	57.4

ECOG indicates Eastern Cooperative Oncology Group; PS, performance status; GTR, macroscopic (gross) total removal; TMZ, temozolomide.

Tumor samples and DNA Extraction

All patients provided their written informed consent for molecular studies of their tumor, and the protocol was approved by the ethics committee at each center. Sixty-eight brain tumor specimens were obtained at the time of first surgical resection.

Tumor tissue samples were immediately frozen and stored at −80°C until the extraction of genomic DNA. DNA was prepared using the QIAmp DNA Mini kit (Qiagen, Hilden, Germany) according to the manufacturer's instructions. Placental DNA was used as the normal control. The amount of DNA obtained from the tumor was sufficient for the subsequent genomic and epigenomic analyses.

Multiplex Ligation-Dependent Probe Amplification

Multiplex ligation-dependent probe amplification (MLPA) was used for the determination of allelic losses and gains of the gene in the tumor samples. The analysis was performed using the SALSA MLPA KIT P088-B1 and P105-C1 in accordance with the manufacturer's protocol (MRC Holland, Amsterdam, Netherland).[12-15] Information regarding the probe sequences and ligation sites can be found at www.mlpa.com. Amplification products were separated on an ABI® 3130 × I Genetic Analyzer (Applied Biosystems, Foster City, CA) and quantified with Genemapper 4.0 software (Applied Biosystems). Duplicate experiments were performed to obtain accurate MLPA values. Data analysis was performed with an original Excel-based program based on MRC-Holland's procedures. Normalization for sample data was first performed on control probes, and each tumor sample was then normalized using the data on 2 control samples, using peripheral blood DNA. Single regression for control and tumor data slope correction was performed. Abnormal/normal ratio limits were set at 0.65 and 1.3. Statistical analysis was performed using the same Coffalyser software.

Pyrosequencing

Tumor DNA was modified with bisulfate using the EpiTect bisulfite kit (Qiagen, Courtaboeuf Cedex, France). Pyrosequencing technology was used to determine the methylation status of the CpG island region of MGMT as described previously.[16,17] We used the touchdown PCR method. The primer sequences used were the MGMT forward primer, 5′-TTGGTAAATTAAGGTATAGAGTTTT-3′, and the MGMT biotinylated reverse primer, 5′-AAA CAATCTACGCATCCT-3′. PCR included a denaturation step at 95°C for 30 s, followed by annealing at various temperatures for 45 s, and extension at 72°C for 45 s. After PCR, the biotinylated PCR product was purified as recommended by the manufacturer. In brief, the PCR product was bound to Streptavidin Sepharose HP (Amersham Biosciences, Uppsala, Sweden), and the Sepharose beads containing the immobilized PCR product were purified, washed, and denatured using 0.2 N NaOH solution and washed again. Next, 0.3 mM pyrosequencing primer was annealed to the purified single-stranded PCR product, and pyrosequencing was performed using the PSQ HS 96 Pyrosequencing System (Pyrosequencing, Westborough, MA). The pyrosequencing primer was 5′-GGAAGTTGGGAAGG-3′. Methylation quantification was performed using the provided software.

TP53 and IDH1/IDH2 Sequencing

Direct sequencing of the *TP53* exons 5 to 8 and *IDH1/IDH2* was performed as previously described.[7,18,19] The primer sequences are listed in Table 2.

Table 2. List of Primer Sequences for Direct DNA Sequencing{TC}

Gene name	Exon		Sequence
TP53	Exon 5	F	5′-TTATCTGTTCACTTGTGCCC-3′
		R	5′-ACCCTGGGCAACCAGCCCTG-3′
	Exon 6	F	5′-ACGACAGGGCTGGTTGCCCA-3′,
		R	5′-CTCCCAGAGACCCCAGTTGC-3′
	Exon 7	F	5′-GGCCTCATCTTGGGCCTGTG-3′
		R	5′-CAGTGTGCAGGGTGGCAAGT-3′
	Exon 8	F	5′-CTGCCTCTTGCTTCTCTTTT-3′
		R	5′-TCTCCTCCACCGCTTCTTGT-3′.
IDH1		F	5′-CGGTCTTCAGAGAAGCCATT-3′
		R	5′-GCAAAATCACATTATTGCCAAC-3′
IDH2		F	5′-AGCCCATCATCTGCAAAAAC-3′
		R	5′-CTAGGCGAGGAGCTCCAGT-3′.

F indicates forward primer; R, reverse primer;.

For IDH sequencing, a fragment 129 bp in length, spanning the sequence encoding the catalytic domain of *IDH1*, including codon 132, and a fragment 150 bp in length spanning the sequence encoding the catalytic domain of *IDH2*, including codon 172, were amplified. We applied touchdown PCR, using the standard buffer conditions: it comprised 5 ng of DNA and AmpliTaq Gold DNA Polymerase (Applied Biosystems) run for 16 cycles with denaturation at 95°C for 30 s, annealing at 65 to 57°C (decreasing by 0.5°C per cycle) for 30 s, and extension at 72°C for 60 s in a total volume of 12.5 μl and add 30 cycles with denaturation at 95°C for 30 s, annealing at 55°C for 30 s, and extension at 72°C for 60 s, ending with at 72°C for 7 min to complete extension.

Direct sequencing was performed using BigDye Terminator v1.1 Cycle Sequencing Kit (Applied Biosystems). The reactions were carried out using an ABI 3100 Genetic Analyzer (Applied Biosystems).

Statistical analysis

Statistical analysis was performed using the statistical software SPSS for Windows, version 17.0 (SPSS Inc, Chicago, Ill). The Mann-Whitney U test, χ^2 test, and Fisher exact test were used to test for association of clinical variables and molecular markers. Survival was estimated by using the Kaplan-Meier method, and survival curves were compared by using the log-rank test. Progression-free survival (PFS) was calculated from the day of first surgery until tumor progression, death, or end of follow up. Overall survival (OS) was calculated from the day of first surgery until death or the end of follow up. Univariate and multivariate analyses were performed to test the potential influence of baseline characteristics on survival. The effect of each single molecular marker on PFS and OS was investigated using the Cox proportional hazards model, adjusting for the major clinical prognostic factors, including age at diagnosis (<40 vs ≥40, <60 vs ≥60 years), ECOG performance status score (ECOG PS; ≤1 vs >1), extent of resection (macroscopic [gross] total resection [GTR] vs non-GTR), tumor location (superficial vs deep), MGMT promoter methylation status, chromosome 1p loss of heterozygosity (LOH), 19qLOH, *PTEN* loss, *CDKN2A* loss, *TP53* loss and mutation, *ERBB2* amplification, *EGFR* amplification, *IDH1* and *IDH2* mutation, and adjuvant therapy (with IFN-β vs without IFN-β). Factors with no significant association with survival, at a level of more than 0.05 in the multivariate analysis, were eliminated. The remaining factors in the multivariate proportional hazard model ($P < .05$) were considered to be independent predictors of survival.

To assess for the treatment effects of TMZ with IFN-β versus TMZ without IFN-β for overall survival (OS), the hazard ratio was computed using a proportional hazard model by baseline characteristics in stratified analysis.

RESULTS

Clinical parameters

Between May 2006 and June 2010, 68 consecutive patients newly diagnosed with primary GBM were registered in this study. Their clinical characteristics are summarized in Table 1. This study group comprised 41 men and 27 women aged 12-84 years (median, 55). The median preoperative ECOG PS score at diagnosis was 1 (range, 0-3); the preoperative ECOG PS score was <1 in 45 patients (66.2%). All tumors were located in the supratentorial region: 50 tumors were located in the superficial area (cortical or subcortical area), and 18 were located in deep anatomical structures such as the basal ganglia and corpus callosum. No tumor was noted in the optic nerve, olfactory nerve, and pituitary gland on pretreatment MRI. No tumor dissemination was detected by MRI. Surgical GTR was achieved in 24 patients (35.3%), and 44 patients underwent non-GTR (64.7%). None of the patients had concurrent active malignancy, and the baseline organ function before chemotherapy was as follows: absolute WBC ≥3000/mm^3 or neutrophil count ≥1,500/mm^3, platelet count ≥100,000/mm^3, hemoglobin ≥8.0 g/dl, AST less than 2.5 × the upper limit of normal (ULN), total bilirubin 2 × ULN, and creatinine 2 × ULN, and electrocardiogram showing no serious

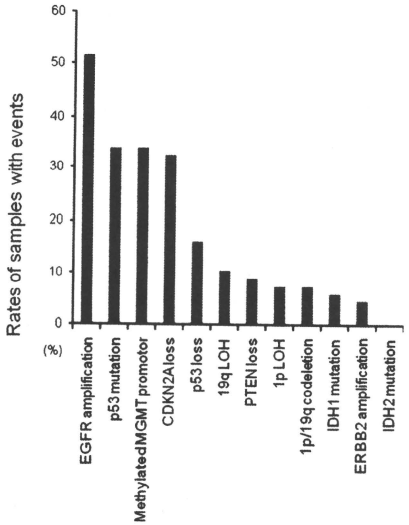

Figure 1. Frequency and pattern of genetic and epigenetic alterations in newly diagnosed primary glioblastoma multiforme (GBM).

arrhythmia and no serious ischemic heart disease. All patients received the standard Stupp regimen,[1] and among these, 39 patients were received combination treatment with IFN-β, as described in the method section.

Frequency of Genetic and Epigenetic Alterations

Of 68 cases, we could obtain sufficient genetic and epigenetic information in all cases. We used direct sequencing for *TP53* and *IDH1/2*. We employed MLPA for the analysis of 1p/19q LOH, loss of *TP53, PTEN* and *CDKN2A*, and amplification of *ERBB2* and *EGFR*. MLPA is a multiplex PCR method that detects abnormal copy numbers of up to 50 different genomic DNA sequences simultaneously. When comparing MLPA to FISH, MLPA not only has the advantage of being a multiplex technique but also one in which very small (50-70 nt) sequences are targeted, enabling MLPA to identify the frequent, single gene aberrations that are very small to be detected by FISH. Furthermore, for the detection of *EGFR* amplification, MLPA can examine exons 1-8, 13, 16, and 22, while previously reported real-time PCR covers only exons 2, 17, and 25. In our preliminary experiments, MLPA was found to be approximately 80% consistent with the real-time PCR method (data not shown). Notably, the methylation status of the MGMT promoter was analyzed by quantitative pyrosequencing technology. Although methylation-specific PCR analysis of MGMT promoter methylation is a widely applicable biomarker for the clinical setting, it is non quantitative and bears a risk of false-positive or false-negative results, especially when the DNA quality and/or quantity is low. Recent attempts to remedy some of these deficiencies have led to the development of an alternative sequence-based approach for methylation analysis, known as pyrosequencing. Pyrosequencing yields continuous methylation values ranging from 0-100%. Based on our comparisons with standard methylation-specific PCR and immunohistochemical study using the anti-MGMT antibody, we determined 14% as the threshold distinguishing unmethylation and methylation of the MGMT promoter in a given tumor.

As indicated in Figure 1 and Table 3, the alterations frequently observed were *EGFR* amplification (51.5%), *TP53* mutation (33.8%), *CDKN2A* loss (32.4%), *TP53* loss (16.2%), methylation of the MGMT promoter (33.8%), and *IDH1* mutation (5.9%). These findings were consistent with those in previous reports.[3,9,20,21]

Clinical, Genetic, and Epigenetic Parameters Associated With Survival in GBM Patients

The median follow-up time was 16.7 months (range, 3.4-46.7 months). The median PFS for all patients was 9.2 months (95% confidence interval [CI], 5.7-12.7). The median OS of all patients was 17.1 months (95% CI, 15.5-18.7) (Figure 2A). The log-rank tests demonstrated that tumor localization ($P = .032$), the MGMT methylation status ($P = .029$), and *TP53* mutation or loss ($P = .035$) were associated with the OS of patients with GBM (Figure 2B-D). These findings were similar to univariate analysis, where deep location ($P = .035$), unmethylated MGMT promoter ($P = .033$) and *TP53* mutation or loss ($P = .038$) were identified as candidate variables for poorer OS (Figure 2). In contrast, well-established prognostic factors such as age, ECOG PS, and the extent of tumor resection did not influence the outcome in this clinical setting. Next, we established multivariate survival models for OS. The model was designed to consider each of these factors without considering the interaction terms. The independent prognostic factors for OS were methylated MGMT promoter ($P = .016$).

Table 3. Relation Between Genetic and Epigenetic Parameters and Overall Survival

Parameter	No.	Months of OS	Log-rank test: *P*
1p LOH			
+	5	16.9	.27
–	63	21.9	
19q LOH			
+	7	17.1	.46
–	61	21.9	
1p/19q codeletion			
+	5	16.9	.27
–	63	21.9	
***PTEN* loss**			
+	6	21.4	.40
–	62	16.9	
***CDKN2A* loss**			
+	22	16.3	.64
–	46	17.4	
***TP53* loss**			
+	11	11.7	**.08**
–	57	17.4	
***ERBB2* amplification**			
+	3	13.9	.77
–	65	17.1	
***EGFR* amplification**			
+	35	17.4	.91
–	33	17.1	
***TP53* mutation**			
+	23	15.7	.128
–	45	17.6	
***TP53* mutation or loss**			
+	29	13.9	**.035**
–	39	17.6	
MGMT promotor			
Unmethylated	45	15.1	**.029**
Methylated	23	21.4	
***IDH1* mutation**			
+	4	19.9	.96
–	64	16.9	
***IDH2* mutation**			
+	0	NA	NA
–	68	NA	

OS indicates overall survival; NA, not available

Combination of IFN-β With TMZ Prolonged Survival

We analyzed whether the use of IFN-β affected the survival of consecutive GBM patients treated with TMZ-based chemotherapy. Of the total 68 patients, 39 (57.4%) received IFN-β in combination of TMZ. Interestingly, the median OS of the combination group was significantly greater with 19.9 months (95% CI, 15.3-24.5) as compared to the TMZ alone group, which was 12.7 months (95% CI, 10.5 to 14.9) (Figure 3A). The 12-month-survival rate was 67.6% for the standard TMZ-treated cohort, whereas it was 83.6% for the combination group. The 24-month survival rates were 22.1% and 34.5%, respectively, for the 2 groups. The difference was statistically significant as determined by the log-rank test and univariate and multivariate analyses.

Benefits of IFN-β for GBM Patients With the Unmethylated MGMT Promoter

Next, we sought to determine the subpopulation that had benefited from the use of the IFN-β combination treatment. It is well known that patients with GBM containing the methylated MGMT promoter benefit from TMZ, but those with the unmethylated MGMT promoter show no such benefits.[1,2] Consistently, the median OS of 45 patients with the unmethylated MGMT status was significantly lesser than that of the patients with the methylated promoter (median OS = 15.1 months; 95% CI, 11.3-18.9). Notably, even in patients whose tumors had the unmethylated MGMT promoter, the median OS was prolonged to 17.2 months (95% CI, 13.9-20.6) when receiving TMZ with IFN-β as compared to the 12.5 months (95% CI, 11.3-13.7) in those receiving TMZ without IFN-β ($P = .017$) (Figure 3B).

Various associations of these clinical and molecular parameters were evaluated. A complete overview of the pairwise associations between these parameters and chemotherapy with or without IFN-β is provided in Figure 4. The relative hazards of OS between TMZ with or without IFN-β groups according to 6 baseline covariates, calculated by means of multivariate analysis, are shown. There were significant associations among patients under 40 years of age ($P = .025$), with ECOG PS ≤ 1 ($P = .004$), deep tumor location ($P = .028$), non-GTR ($P = .048$), and ummethylated MGMT status ($P = .02$) (Figure 4).

DISCUSSION

Genomic Analysis in Newly Diagnosed GBMs

In this study, we analyzed the genomic abnormalities in 68 consecutive newly diagnosed patients with GBM who were treated with TMZ-based chemotherapy. We observed *TP53* mutation (33.8%), *TP53* loss (16.2%), *EGFR* amplification (51.5%), *CDKN2A* loss (32.4%),

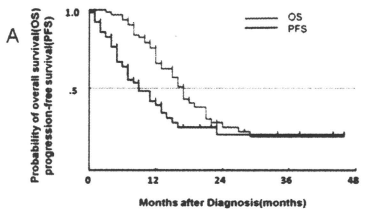

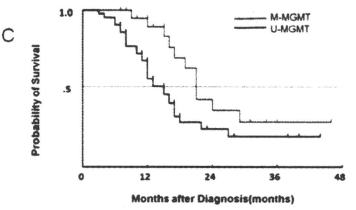

Predictors of overall survival in the subgroup of patients

variable	Log-rank	Univariate analysis			Multivariate analysis		
		HR	95%CI	p	HR	95%CI	p
MGMT promotor							
Unmethylated		1			1		
Methylated	0.029	0.47	0.24 to 0.94	0.033	0.38	0.18 to 0.83	0.016

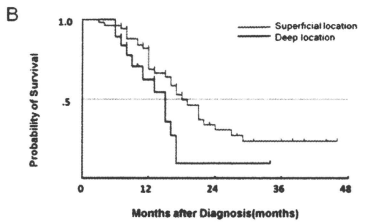

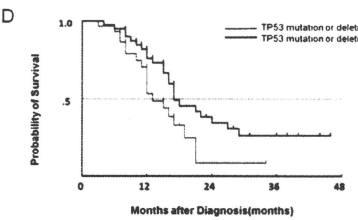

Predictors of overall survival in the subgroup of patients

variable	Log-rank	Univariate analysis			Multivariate analysis		
		HR	95%CI	p	HR	95%CI	p
Tumor location							
superficial		1			1		
deep	0.032	2.09	1.05 to 4.15	0.035	1.9	0.83 to 4.33	0.126

Predictors of overall survival in the subgroup of patients

variable	Log-rank	Univariate analysis			Multivariate analysis		
		HR	95%CI	p	HR	95%CI	p
TP53 mutation or loss							
-		1			1		
+	0.035	1.94	1.04 to 3.62	0.038	1.58	0.74 to 3.38	0.24

Figure 2. Kaplan-Meier curves showing overall survival (OS) and progression-free survival (PFS) for the entire cohort (A), and OS according to (B) tumor location ($P = .032$), (C) MGMT promoter methylation status ($P = .029$), and (D) *TP53* mutation or loss ($P = .035$) (D). Predictors of overall survival in the subgroups of patients by univariate and multivariate analyses were shown (B-D). The hazards ratio (HR) was adjusted for the factors; age, Eastern Cooperative Oncology Group performance status (ECOG PS), the extent of tumor resection, MGMT promoter methylation status, *TP53* mutation or loss and TMZ with or without interferon-β (IFN-β) in the multivariate analysis.

and methylation of the MGMT promoter (33.8%). Recent large-scale efforts to characterize the GBM genome have identified additional alterations in genes not previously implicated in glioma, such as *ERBB2* and *IDH1/IDH2* mutation in primary and secondary GBM, respectively, and a significant incidence of mutation and genomic loss of *NF1*.[3,4,6] The TCGA study also noted *TP53* mutations and losses in 35% of the cases, which is a surprisingly higher frequency than that reported previously.[3,20,21] Furthermore, this study also revealed *EGFR* amplification (45%), *CDKN2A* loss (52.0%), and methylation of the MGMT promoter (20.9%). These results were consistent with our data. *IDH1* mutations have recently been identified in gliomas, which are a strong predictor of a more favorable prognosis.[6] Our study supported the finding that within the group of primary GBM, *IDH1* mutations are rare and tend to define a prognostically favorable outcome.

Factors for Prognosis and Prediction of Response to Therapy

The current study demonstrated that the methylated MGMT promoter and the combination of IFN-β and TMZ were independent prognostic indicators of GBM patients on multivariate analysis. Epigenetic silencing by the MGMT promoter methylation correlates with improved survival in glioma patients treated with TMZ.[2,22-25] The prognostic significance of MGMT promoter methylation has been shown in several clinical trials. In these studies, MGMT promoter methylation was an independent favorable prognostic factor and patients whose tumor contained a methylated MGMT promoter

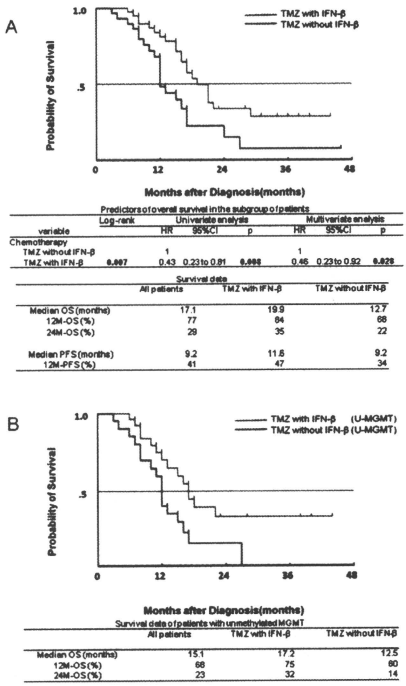

Figure 3. Kaplan-Meier estimates of overall survival (OS) according to temozolomide (TMZ) with or without interferon-β (IFN-β) for all patients (A) ($P = .007$) and for patients with unmethylated MGMT promoter (U-MGMT) (B) ($P = .017$). The hazards ratio (HR) was adjusted for the factors; age, Eastern Cooperative Oncology Group performance status (ECOG PS), the extent of tumor resection, MGMT promoter methylation status, *TP53* mutation or loss, and TMZ with or without IFN-β in the multivariate analysis.

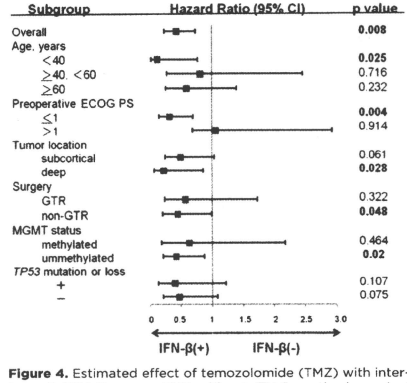

Figure 4. Estimated effect of temozolomide (TMZ) with interferon-β (IFN-β) versus TMZ without IFN-β on the hazard of overall survival (OS), according to baseline characteristics. The hazard ratio was computed using a proportional hazard model by selected factors. There were significant associations under 40 years of age (age, <40), with Eastern Cooperative Oncology Group performance status (ECOG PS) ≤1, deep tumor location, no macroscopic (gross) total resection (non-GTR), and ummethylated MGMT status.

showed overall prolonged survival when treated with TMZ and radiotherapy. Our results demonstrated similarly that MGMT promoter hypermethylation determined by a novel pyrosequencing technology was significantly associated with better OS.

There are several contradicting reports on survival related to the prognostic value of *TP53* mutations in GBM, showing either no association or that the presence of *TP53* mutations was a favorable or an unfavorable prognostic factor.[9,20,21,26] On the other hand, our results demonstrated that *TP53* mutation or loss was significantly associated with poor OS only in univariate analysis, but not in multivariate analysis. These findings were not in conflict with recent evidence, which shows that *TP53* mutations not only disrupt its function but also possess gain-of-function and dominant-negative effects on the wild-type p53 protein, thus making the mutated *TP53* gene an oncogene.[27]

Benefits of IFN-β and TMZ combination treatment for GBM

The current study demonstrated that newly diagnosed primary GBM patients were associated with a favorable outcome on IFN-β and TMZ combination chemotherapy. The IFN-β and TMZ combination group achieved a median OS of 19.9 months (Figure 3A). This excellent result was almost equal to the median OS of only patients with the methylated MGMT promoter in the EORTC/NCIC trial.

IFN-β elicits pleiotropic biological effects such as antiproliferation, immunomodulation, and cell differentiation.[28] Furthermore, it has been widely used either alone or in combination with other antitumor agents in the treatment of malignant brain tumors and melanomas. In our previous studies, we showed that combination therapy with

IFN-β and nitrosourea has been particularly useful in the treatment of malignant gliomas in Japan.[10] IFN-β has multifaceted functions related to antitumor activity, such as cytostatic effects, participating in the differentiation of CTLs and potentiation of their antitumor immunological responses, and behavior as a drug sensitizer to enhance toxicity against various malignant neoplasms when administered in combination with nitrosourea.[10] Previously, in an in vitro study, we corroborated that IFN-β markedly enhanced chemosensitivity to TMZ[29]; this manifestation revealed that one of the major mechanisms by which IFN-β enhances chemosensitivity is the down-regulation of MGMT transcription. This effect was also confirmed in an experimental animal model.[30] A subanalysis in this study showed that patients whose tumor had an unmethylated promoter benefited from the addition of IFN-β, suggesting that the combination of IFN-β and TMZ might provide better clinical outcomes in patients with the unmethylated MGMT promoter (Figures 3B, 4). Although we discovered that the patients under 40 years of age at diagnosis and those who had an initial ECOG PS ≤ 1 seemed to receive the benefit from IFN-β and TMZ combination therapy, our phase I study revealed that the combination regimen of IFN-β and TMZ was safe and well tolerated even in patients with older age and worse PS (Figure 4; manuscript in submission). In addition, the benefit associated with IFN-β was shown in patients whose tumors were deep, who had undergone non-GTR (Figure 4). This finding suggests that IFN-β might be better for use in cases of complicated tumor removal, i.e., when the tumors were deep, all the tumors could not be removed because they were, for example, located in an eloquent area or around essential structures.

In summary, this study supported the hypothesis that in cases of newly diagnosed primary GBM, IFN-β and TMZ combination therapy was significantly associated with a favorable outcome. To our knowledge, this is the first study to associate the survival benefits derived from IFN-β and TMZ combination. These benefits were, in particular, well correlated in patients with an unmethylated MGMT promoter.

Our results are limited as opposed to a prospective clinical trial as retrospective studies might have been influenced by unrecognized biases. However, the subject group we used was a consecutive series of patients, and this study provides novel information on the treatment for GBM. Thus, accumulation of evidence for this treatment will help further improvement of this disease and hopefully become a novel therapy. We are planning a prospective randomized control trial to compare the clinical outcomes between TMZ alone and a combination of TMZ and IFN-β in newly diagnosed GBM patients.

CONFLICT OF INTEREST DISCLOSURES

This work was supported by grants from a Grant-in-Aid (C) for Scientific Research from the Ministry of Health, Labor, and Welfare, Japan (A.N.).

REFERENCES

1. Stupp R, Mason WP, van den Bent MJ, et al. Radiotherapy plus concomitant and adjuvant temozolomide for glioblastoma. *N Engl J Med.* Mar 10 2005;352(10):987-996.
2. Hegi ME, Diserens AC, Gorlia T, et al. MGMT gene silencing and benefit from temozolomide in glioblastoma. *N Engl J Med.* Mar 10 2005;352(10):997-1003.
3. Comprehensive genomic characterization defines human glioblastoma genes and core pathways. *Nature.* Oct 23 2008;455(7216):1061-1068.
4. Parsons DW, Jones S, Zhang X, et al. An integrated genomic analysis of human glioblastoma multiforme. *Science.* Sep 26 2008;321(5897):1807-1812.
5. Yan H, Bigner DD, Velculescu V, Parsons DW. Mutant metabolic enzymes are at the origin of gliomas. *Cancer Res.* Dec 15 2009;69(24):9157-9159.
6. Yan H, Parsons DW, Jin G, et al. IDH1 and IDH2 mutations in gliomas. *N Engl J Med.* Feb 19 2009;360(8):765-773.
7. Nobusawa S, Watanabe T, Kleihues P, Ohgaki H. IDH1 mutations as molecular signature and predictive factor of secondary glioblastomas. *Clin Cancer Res.* Oct 1 2009; 15(19):6002-6007.
8. Kleihues P BP, Collins VP, et al, ed. WHO Classification of Tumours of the Central Nervous System. Lyon: WHO Press; 2000. IARC,ed.
9. Louis DN, Ohgaki H, Wiestler OD, et al. The 2007 WHO classification of tumours of the central nervous system. *Acta Neuropathol.* Aug 2007;114(2):97-109.
10. Wakabayashi T, Hatano N, Kajita Y, et al. Initial and maintenance combination treatment with interferon-beta, MCNU (Ranimustine), and radiotherapy for patients with previously untreated malignant glioma. *J Neurooncol.* Aug 2000;49(1):57-62.
11. Wakabayashi T, Kayama T, Nishikawa R, et al. A multicenter phase I trial of interferon-beta and temozolomide combination therapy for high-grade gliomas (INTEGRA Study). *Jpn J Clin Oncol.* Oct 2008;38(10):715-718.
12. Franco-Hernandez C, Martinez-Glez V, Alonso ME, et al. Gene dosage and mutational analyses of EGFR in oligodendrogliomas. *Int J Oncol.* Jan 2007;30(1):209-215.
13. Jeuken J, Cornelissen S, Boots-Sprenger S, Gijsen S, Wesseling P. Multiplex ligation-dependent probe amplification: a diagnostic tool for simultaneous identification of different genetic markers in glial tumors. *J Mol Diagn. Sep* 2006; 8(4):433-443.
14. Schouten JP, McElgunn CJ, Waaijer R, Zwijnenburg D, Diepvens F, Pals G. Relative quantification of 40 nucleic acid sequences by multiplex ligation-dependent probe amplification. *Nucleic Acids Res.* Jun 15 2002;30(12):e57.

15. Martinez-Glez V, Franco-Hernandez C, Lomas J, et al. Multiplex ligation-dependent probe amplification (MLPA) screening in meningioma. *Cancer Genet Cytogenet.* Mar 2007;173(2):170-172.
16. Natsume A, Wakabayashi T, Tsujimura K, et al. The DNA demethylating agent 5-aza-2′-deoxycytidine activates NY-ESO-1 antigenicity in orthotopic human glioma. *Int J Cancer.* Jun 1 2008;122(11):2542-2553.
17. Oi S, Natsume A, Ito M, et al. Synergistic induction of NY-ESO-1 antigen expression by a novel histone deacetylase inhibitor, valproic acid, with 5-aza-2′-deoxycytidine in glioma cells. *J Neurooncol.* Mar 2009;92(1):15-22.
18. Fults D, Brockmeyer D, Tullous MW, Pedone CA, Cawthon RM. p53 mutation and loss of heterozygosity on chromosomes 17 and 10 during human astrocytoma progression. *Cancer Res.* Feb 1 1992;52(3):674-679.
19. Hartmann C, Meyer J, Balss J, et al. Type and frequency of IDH1 and IDH2 mutations are related to astrocytic and oligodendroglial differentiation and age: a study of 1,010 diffuse gliomas. *Acta Neuropathol.* Oct 2009;118(4):469-474.
20. Ohgaki H, Dessen P, Jourde B, et al. Genetic pathways to glioblastoma: a population-based study. *Cancer Res.* Oct 1 2004;64(19):6892-6899.
21. Weller M, Felsberg J, Hartmann C, et al. Molecular predictors of progression-free and overall survival in patients with newly diagnosed glioblastoma: a prospective translational study of the German Glioma Network. *J Clin Oncol.* Dec 1 2009;27(34):5743-5750.
22. Hegi ME, Liu L, Herman JG, et al. Correlation of O6-methylguanine methyltransferase (MGMT) promoter methylation with clinical outcomes in glioblastoma and clinical strategies to modulate MGMT activity. *J Clin Oncol.* Sep 1 2008;26(25):4189-4199.
23. Chinot OL, Barrie M, Fuentes S, et al. Correlation between O6-methylguanine-DNA methyltransferase and survival in inoperable newly diagnosed glioblastoma patients treated with neoadjuvant temozolomide. *J Clin Oncol.* Apr 20 2007;25(12):1470-1475.
24. Eoli M, Menghi F, Bruzzone MG, et al. Methylation of O6-methylguanine DNA methyltransferase and loss of heterozygosity on 19q and/or 17p are overlapping features of secondary glioblastomas with prolonged survival. *Clin Cancer Res.* May 1 2007;13(9):2606-2613.
25. Esteller M, Garcia-Foncillas J, Andion E, et al. Inactivation of the DNA-repair gene MGMT and the clinical response of gliomas to alkylating agents. *N Engl J Med.* Nov 9 2000; 343(19):1350-1354.
26. Ruano Y, Ribalta T, de Lope AR, et al. Worse outcome in primary glioblastoma multiforme with concurrent epidermal growth factor receptor and p53 alteration. *Am J Clin Pathol.* Feb 2009;131(2):257-263.
27. Waldman YY, Tuller T, Sharan R, Ruppin E. TP53 cancerous mutations exhibit selection for translation efficiency. *Cancer Res.* Nov 15 2009;69(22):8807-8813.
28. Borden EC, Sen GC, Uze G, et al. Interferons at age 50: past, current and future impact on biomedicine. *Nat Rev Drug Discov.* Dec 2007;6(12):975-990.
29. Natsume A, Ishii D, Wakabayashi T, et al. IFN-beta down-regulates the expression of DNA repair gene MGMT and sensitizes resistant glioma cells to temozolomide. *Cancer Res.* Sep 1 2005;65(17):7573-7579.
30. Natsume A, Wakabayashi T, Ishii D, et al. A combination of IFN-beta and temozolomide in human glioma xenograft models: implication of p53-mediated MGMT down-regulation. *Cancer Chemother Pharmacol.* Apr 2008;61(4): 653-659.

Neuroscience Letters 485 (2010) 65–70

Contents lists available at ScienceDirect

Neuroscience Letters

journal homepage: www.elsevier.com/locate/neulet

A free-radical scavenger protects the neural progenitor cells in the dentate subgranular zone of the hippocampus from cell death after X-irradiation

Kazuya Motomura[a,1], Masatoshi Ogura[a,1], Atsushi Natsume[a,b,*], Hidenori Yokoyama[a], Toshihiko Wakabayashi[a]

[a] Department of Neurosurgery, Nagoya University School of Medicine, Japan
[b] Center for Genetic and Regenerative Medicine, Nagoya University School of Medicine, Japan

ARTICLE INFO

Article history:
Received 9 April 2010
Received in revised form 3 August 2010
Accepted 22 August 2010

Keywords:
Free-radical scavenger
X-irradiation
Neural stem cells
Hippocampus

ABSTRACT

It has been elucidated that cognitive dysfunction following cranial radiotherapy might be linked to the oxidative stress-induced impairment of hippocampal neurogenesis that is mediated by proliferating neural stem or progenitor cells. The novel free-radical scavenger edaravone (3-methyl-1-phenyl-2-pyrazolin-5-one) has been clinically used to reduce neuronal damage following ischemic stroke. Previously, we reported that the free-radical scavenger, edaravone, which is currently used to treat patients with brain ischemia, protected cultured human neural stem cells (NSCs) from radiation-induced cell death; the protective effect was observed more significantly in NSCs than in brain tumor cells. Here, in animal models, we demonstrate that edaravone protects neurons in the subgranular zone (SGZ) of the dentate gyrus of the hippocampus from cell death after irradiation. Moreover, edaravone protected spatial memory retention deficits as determined by Morris water maze tests. Our study may shed some light on the beneficial effects of free-radical scavengers in impaired neurogenesis following cranial radiation therapy.

Cranial radiation therapy is widely used to treat primary and metastatic brain tumors and head and neck cancers. Patients who receive radiotherapy that involves the brain frequently experience a progressive cognitive decline [1,4]. Although white matter necrosis and vasculopathy are overt pathologies caused by radiation-induced injury [15], little is known about the underlying mechanism of learning and memory deficits. Several reports demonstrated the relationship between radiation-induced cognitive dysfunction and apoptosis in hippocampal neurons because of oxidative stress [12,20]. Furthermore, it was reported that ionizing radiation delivered in a single 10 Gy dose of X-rays to the rat brain selectively kills a histomorphologically well-defined population of proliferating cells in the subgranular zone (SGZ) of the dentate gyrus [19]. Other researchers reported that SGZ apoptosis peaked 12 h after irradiation and then continued for 48 h [13]. Moreover, it has been suspected that the newly generated neurons in this region contribute to hippocampal function and that adult hippocampal neurogenesis can be correlated with spatial pattern separation [3].

Previously, we demonstrated that a free-radical scavenger, edaravone, protected human neural stem cells (NSCs) from radiation-induced cell death [11]. Free radicals are highly reactive chemical species and differ from all other species in that they possess an unpaired electron; this electron becomes paramagnetic and relatively reactive [2,5]. It has been observed that free radicals attack polyunsaturated fatty acids of membrane lipids *in vivo*, which results in the oxidative deterioration of membrane lipids; this is known as lipid peroxidation [9,10]. One of the important radiation-induced free-radical species is the hydroxyl radical that indiscriminately attacks neighboring molecules, often at near-diffusion-controlled rates [21]. Hydroxyl radicals are generated by ionizing radiations, either directly by oxidation of water or indirectly by formation of secondary partially reactive oxygen species, including superoxide, hydroxyl, and nitric oxide (NO) radicals. Edaravone interacts biochemically with a wide range of free radicals, donates electrons, and eventually transforms itself to the stable compound, 2-oxo-3-(phenylhydrazono)-butanoic acid (OPB). The agent also exerts pharmacological neuroprotective effects in the case of brain ischemia by decreasing the levels of inducible NO synthase (iNOS) [22,23]. Although edaravone has been reported to inhibit endothelial injury and neuronal damage in brain ischemia, it remains unclear whether it can effectively prevent radiation-induced brain injury. The aim of this study was to investigate whether edaravone can exert protective and anti-apoptotic effects on neurogenesis and cognitive function in mice

* Corresponding author at: Department of Neurosurgery, Nagoya University School of Medicine, 65 Tsurumai-cho, Showa-ku, Nagoya 466-8550, Japan. Tel.: +81 52 744 2353; fax: +81 52 744 2360.
E-mail address: anatsume@med.nagoya-u.ac.jp (A. Natsume).
[1] These authors contributed equally to this study.

0304-3940/$ – see front matter © 2010 Elsevier Ireland Ltd. All rights reserved.
doi:10.1016/j.neulet.2010.08.065

that were irradiated at young age. Our results show that edaravone protects the neurons in SGZ of the dentate gyrus in young mice from radiation-induced cell death.

Male 3-week-old C57BL/J6 mice (SLC, Shizuoka, Japan) were used in all experiments. All experiments were performed in accordance with the Guidelines for Animal Experiments of Nagoya University Graduate School of Medicine.

Edaravone was kindly provided by the Mitsubishi-Tanabe Pharma Corporation (Osaka, Japan). We dissolved 30 mg of edaravone in 500 μl of 1 N NaOH, added 8 ml distilled water, and then adjusted the pH to 7 with 1 N HCl. The final concentration of edaravone was adjusted to 3.0 mg/ml. Mice were irradiated by using an X-ray generator (MBR-1520-3; Hitachi) at 125 kVp and 20 mA, with a filter of 0.5 mm aluminum and 0.2 mm copper. The dose rate was approximately 2.0–2.3 Gy/min. Mice were anesthetized by an intraperitoneal injection of pentobarbital [50 mg/kg body weight (BW)]; sham-irradiated mice (control) were only anesthetized. The cranial X-irradiation beam was directed down onto the head at a source-to-skin distance of 10 cm, while their bodies were shielded with 0.6 mm-thick lead. Mice were housed individually after irradiation in order to minimize the effect of social influences on behavioral tests. Furthermore, mice were injected intraperitoneally with edaravone (3.0 or 6.0 mg/kg BW) 30 min before X-irradiation.

In order to determine the optimal irradiation dose that induces apoptosis in neurons in the SGZ, irradiation of 0, 5, 7.5, or 10 Gy was given to the mouse brain, and brain tissues were collected 48 h later. Sham-irradiated mice were also sacrificed at that time. For tissue collection, mice were deeply anesthetized, and 50 ml of 4% buffered formalin fixative solution was transcardially infused. After 5 min, the brain was removed and immersed in 4% buffered formalin solution for 3 days. Fixed brains were cut coronally at the parieto-occipital junction, thereby providing elongated exposure of each hippocampus.

Apoptosis-positive cells were stained with the MEBSTAIN Apoptosis kit II according to the instructions of the manufacturer (MBL, Nagoya, Japan). We used the anti-neuronal-specific beta-III tubulin antibody (TuJ-1; R&D Systems, Minneapolis, USA) and Alexa Fluor 546 secondary antibodies (Molecular Probes, Eugene, OR, USA) for counterstaining. Following deparaffinization and antigen retrieval using proteinase K, sections were incubated for 30 min in 0.25% Triton X-100/PBS, followed by incubation in 1% gelatin/PBS for 30 min. The sections were washed several times with PBS and incubated at room temperature for 50 min with TuJ-1 (5 μg/ml). Thereafter, the TUNEL reaction mixture was added to the sections and incubated for 10 min at room temperature. The sections were then incubated with the mixture of FITC-dUTP and Alexa Fluor 546 secondary antibodies (1:500) for 1 h in the dark, and then washed with PBS. The number of TUNEL-labeled cells was counted and averaged in bilateral blades in the SGZ. The total number of apoptotic cells was determined by summing the values from all 3 non-overlapping sections for each mouse. All positively labeled cells within the SGZ of the dentate gyrus were quantified by 2 independent observers. The numbers of TUNEL-positive cells were represented as the mean ± SD, and differences among means were evaluated by analysis of variance (ANOVA) (SPSS; SPSS Inc., Chicago, IL, USA). A value of $p < 0.01$ was considered statistically significant.

The novel object recognition test was carried out on 3 consecutive days 48 h after X-irradiation as previously described with slight modifications [7,18]. The apparatus consisted of an open plastic box (30 cm × 30 cm × 30 cm), the outside of which was covered with a black plastic film. The mice were individually habituated in the open box (with no object for 5 min) for 2 days. The mice were tested on the 3rd day. The task consisted of the sample phase and the choice phase. At the start of the sample phase, 2 identical objects (A1 and A2) were placed in the box, 5 cm from the side wall. A mouse was then placed in the box. The total time that the mouse spent exploring the 2 objects was recorded by the experimenter with 2 stopwatches. Exploration of an object was defined as directing the nose to the object at a distance of less than 1 cm and/or touching it with the nose. The mouse was placed back in its home cage after 7 min had elapsed. Fifteen minutes after the sample phase, the mice were reintroduced into the open field for 7 min (choice phase). In this phase, 1 of the familiar objects (A2) was replaced by a new object (B). The time that the mouse spent exploring object B was recorded. The values were represented as percentage time spent for object B of the total time spent for the objects A2 + B.

Morris water maze test was performed as previously described [17]. The circular water tank (60 cm in diameter, 25 cm high) had 4 equally spaced quadrants (north, south, east, and west). First, the mice were trained to locate a visible platform (5 cm in diameter, surface 1 cm above the surface of the water; days 1 and 2), and then a submerged hidden platform (transparent, 5 cm in diameter, surface 2–5 mm below the surface of the water; days 3–5) in 2 daily sessions (3.5 h apart). Each session consisted of 3 trials (60 s each; 10 min intervals). Mice that failed to find the hidden platform within 60 s were placed onto the platform for 15 s. During the training with the visible platform, the platform was moved to a different quadrant in each session. During the training with the hidden platform, the platform was placed in the center of the target quadrant and always kept there for each mouse. The starting point at which the mouse was placed into the water was changed in each trial. The experimenter recorded the time to reach the platform (latency) in each trial. Statistical analysis for behavioral studies was performed using the one-way and two-way analysis of variance (ANOVA) followed by Bonferroni test. A value of $p < 0.05$ was considered statistically significant. Data were expressed as means ± SD.

We determined the optimal radiation dose that induced apoptosis and the timing of observation in the SGZ by exposing 3-week-old mice to various doses (0, 5, 7.5, and 10 Gy) of cranial irradiation. Coronal sections of the brain (including the hippocampus) were analyzed for apoptosis using TUNEL staining. While the number of TUNEL-positive cells observed along the basal layer of the bilateral dentate gyrus (i.e., SGZ) was limited in control group (Fig. 1A, F, 4.8 ± 1.0 cells) and the groups that received 5 Gy (Fig. 1B, F, 11.2 ± 2.8 cells), and 7.5 Gy (Fig. 1C, F, 13.5 ± 2.5 cells), it was significantly increased by 10 Gy-irradiation (Fig. 1D, F, 74.9 ± 3.9 cells, $p < 0.01$). However, we could observe few TUNEL-positive cells at 24 h even after 10 Gy-irradiation (Fig. 1E). Therefore, we concluded that an irradiation dose of 10 Gy induced cell death at 48 h in the SGZ effectively.

In order to assess the effect of edaravone on X-ray-induced apoptosis, mice were treated with edaravone at a final concentration of 0, 3.0, or 6.0 mg/kg BW 30 min prior to X-irradiation. TUNEL staining was performed 48 h after X-irradiation to detect and analyze apoptosis. There was a statistical significance in the difference of TUNEL-positive cells between the group that received only irradiation (Fig. 2A, 74.9 ± 3.9 cells) and the group that received 3.0 mg/kg edaravone (Fig. 2B, 53.6 ± 6.1 cells) ($p < 0.05$). The difference was more dramatic between the group that received only irradiation and the group that received 6.0 mg/kg edaravone (Fig. 2C, 40.6 ± 4.0 cells) ($p < 0.01$). The number of TUNEL-positive cells significantly decreased in the group that received 6.0 mg/kg edaravone (Fig. 2D).

On the basis of these results on the cell injury assessment, a dose of 6.0 mg/kg edaravone was given in two behavioral tests; novel object recognition test and Morris water maze test.

Novel object recognition test was performed to evaluate the hippocampus- and cortex-dependent non-spatial learning and memory (Fig. 3). All mice spent more time exploring the new object (B) than the familiar object (A2), but there was no difference between the groups (in sample phase, control: 48.9 ± 3.0%, irradiated without treatment: 52.3 ± 1.9%, irradiated with treatment of 6 mg/kg of edaravone: 48.3 ± 2.3%, in the choice phase, control:

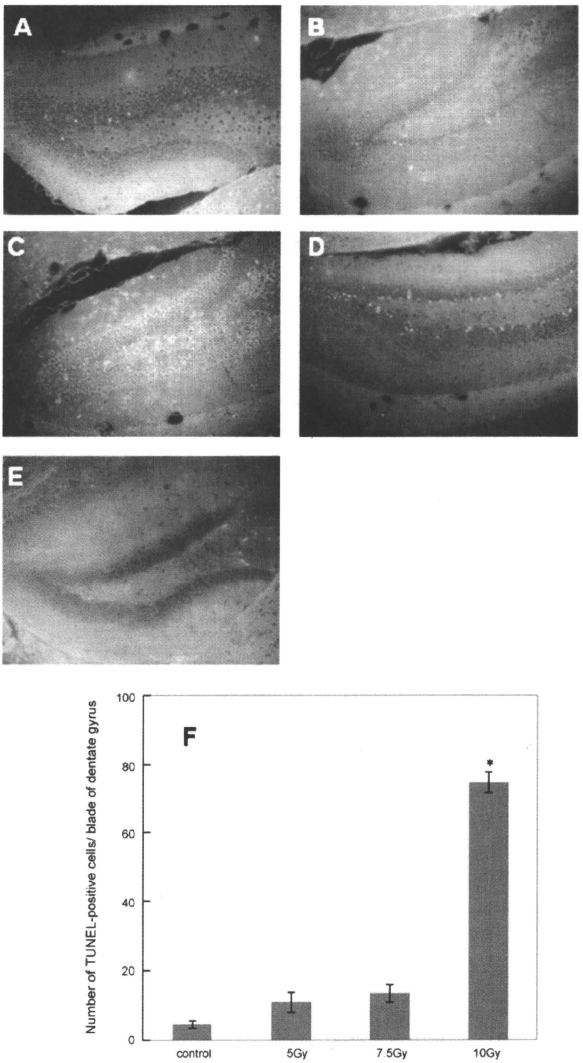

Fig. 1. Double staining of the dentate gyrus of the hippocampus with TUNEL (green) and neuron-specific beta-III tubulin antibody (red) before irradiation (A) and 48 h after X-irradiation with 5 Gy (B), 7.5 Gy (C), 10 Gy (D), and 24 h after 10 Gy-irradiation (E). Occasional TUNEL-positive cells were seen in tissues from non-irradiated mice (control, A). There were no differences between any 2 groups of control, 5, and 7.5 Gy. Compared with those groups, a significant increase of TUNEL-positive cells was seen in the SGZ after irradiation with 10 Gy ($^*p < 0.01$) (F). All micrographs are at 200× magnification. Values are presented as mean ± SEM. The statistical significance of difference was determined by analysis of variance (ANOVA).